Interface formation of GaAs with Si(100), Si(111), and Ge(111): Core-level spectroscopy for monolayer coverages of GaAs, Ga, and As

R. D. Bringans, M. A. Olmstead,* R. I. G. Uhrberg,† and R. Z. Bachrach
Xerox Palo Alto Research Center, 3333 Coyote Hill Road, Palo Alto, California 94304
(Received 18 June 1987)

The interface structure of thin overlayers of GaAs grown using molecular-beam epitaxy techniques on on-axis Si(100), Si(111), and Ge(111) substrates has been studied using photoemission core-level spectroscopy. Results for As and Ga overlayers are also reported and are utilized to interpret the results for GaAs growth. The interface bonding is found to be the same for growth using predeposition of Ga as for predeposition of As. For GaAs on Si(111), the bonding at the interface is found to consist predominantly of Si—As bonds. We also find strong evidence of island formation before the completion of the first GaAs bilayer. The total area between islands can be reduced either by faster deposition rates or by using a Ga prelayer. For GaAs on Si(100), bonding takes place to both Ga and As but with fewer Si—Ga bonds than Si—As bonds. The tendency to island formation is less than for the Si(111) case. These results are compared with earlier data for As interaction with off-axis Si(100) surfaces to explain the absence of antiphase domains in GaAs grown on off-axis (100) substrates. Roughly equal numbers of Ge—As and Ge—Ga bonds were found for GaAs on Ge(111), and this result is interpreted as indicating that Ge interdiffuses more rapidly into GaAs than does Si.

I. INTRODUCTION

The heteroepitaxy of compounds on elemental semiconductors poses many interesting questions about interface formation. The foremost of these concerns the nature of the chemical bonds at the interface and the related atomic arrangement. In this study of GaAs heteroepitaxy on Si and Ge substrates, the bulk materials are particularly well understood, allowing us to concentrate on new effects of the interface alone. The GaAs-on-Si material system has also been shown to have significant technological promise as a means of combining silicon integrated circuits with the optical and electronic performance of the III-V compounds. GaAs of sufficient quality to fabricate working devices such as bipolar transistors, solar cells, and heterojunction lasers (see, for example, Refs. 1, 2, and 3, respectively) has been grown on Si(100) substrates using both molecular-beam epitaxy (MBE) and metal-organic chemical-vapor deposition (MOCVD). The large number of dislocations in the GaAs produced in this way, however, leads to potential problems of reliability and long-term stability, particularly for laser structures.[4] The present study addresses some of these issues by examining the beginning of MBE-grown GaAs on Si and Ge substrates.

Interface chemistry is qualitatively different from that in the bulk of Si, Ge, or GaAs and so it is not straightforward to make simple estimates of the atomic structure of the interfaces between these materials. The effects of the polarity of GaAs, lattice mismatch, interdiffusion between the overlayer and the substrate, and three-dimensional rather than layer-by-layer growth of GaAs need to be addressed. To explain some of these points, Fig. 1 shows a *simplified* reference model of the atomic structure of GaAs overlayers on the (100) and (111) surfaces of Si or Ge. In the figure, all interface bonding is shown between Si and As atoms and the GaAs is assumed to grow pseudomorphically without misfit dislocations. The left-hand side of the figure shows the structures determined previously[5–8] for arsenic overlayers on the two surfaces.

Photoemission core-level spectroscopy coupled with spectroscopic deconvolution provides the principal results presented in this study of the evolution of MBE-grown GaAs overlayers on Si and Ge. This method is particularly suitable for the investigation of interface formation because it is sensitive to the chemical environment around each atom and has a probe depth which can be varied from a few monolayers to around 20 monolayers. After a description of the experimental method used, results for isolated As and Ga layers on Si and Ge substrates will be discussed. These results will then be compared to those for GaAs overlayers on the same surfaces.

In the on-axis [100] and [111] directions of growth studied here, GaAs is polar, consisting of alternating layers of Ga and As atoms. It has been suggested[9] that this will cause atomic rearrangements at the interface to reduce the interface dipole caused by bonding of the substrate to Ga or As alone. It is thus of interest to determine whether As alone, Ga alone, or both Ga and As bond to Si or Ge at the interface. We have made a comparative study of the nature of the interface bonding for As, Ga, and GaAs with Si(111), Si(100), and Ge(111) surfaces. Use of these different substrates has allowed us to vary the geometry at the interface as well as the magnitude of the lattice mismatch and the tendency for interdiffusion to occur. We will also discuss the implica-

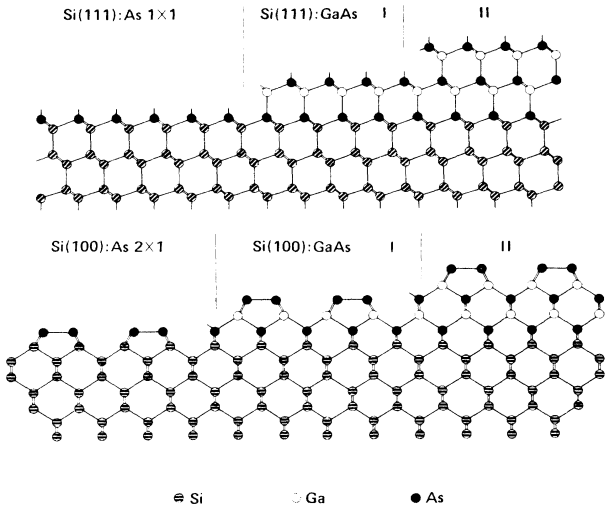

FIG. 1. The upper portion of the figure shows the structure of the Si(111):As (1×1) surface and a *simplified* model of the Si(111) surface with overlayers of different thicknesses of GaAs. The same structural models apply when the substrate is Ge(111). The lower portion shows the structure of Si(100):As (2×1) and a *simplified* model of the Si(100) surface with overlayers of different thicknesses of GaAs.

tions of results[10] for interaction of As with off-axis Si(100) surfaces in terms of our models of the GaAs-on-Si(100) interface. It has been shown[11] that use of off-axis Si(100) substrates improves the quality of subsequently grown GaAs.

We have found in our study that (i) well-resolved core-level shifts exist for the As-terminated surfaces and deconvolution of core-level line shapes shows that only a single As site and a single Si or Ge interface site are present on each surface; (ii) the interface bonding between GaAs and the substrate is the same for growth using predeposition of Ga as for predeposition of As; (iii) the stability of the As-terminated surfaces leads to island formation at the beginning of GaAs growth; (iv) the area between islands on Si(111) can be reduced at faster deposition rates or if a Ga prelayer is used; (v) in the case of GaAs on Si(111), the core-level shifts are well resolved and allow us to conclude that bonding of the substrate occurs predominantly to As atoms; (vi) for Ge(111), bonding appears to be to both As and Ga; and (vii) the results for GaAs on Si(100) are more difficult to interpret, but indicate that a significant area of the substrate is covered by GaAs at equivalent coverages of around one double layer of GaAs.

II. EXPERIMENTAL DETAILS AND DATA REDUCTION

The Si(111) (p-type, 10 Ω cm), Si(100) (n-type, 0.5 Ω cm), and Ge(111) (p-type, 0.5 Ω cm) substrates were aligned to within 0.5° of their nominal direction, and polished with alumina and then with a colloidal suspension of silica.[12] After introduction into the vacuum chamber they were sputtered with 500-eV Ar^+ ions and then annealed by passing a direct current through them. Auger and core-level spectroscopies were used to check contamination and low-energy electron diffraction (LEED) was used to check the surface order. Sharp $c(2\times8)$, (7×7), and (2×1) LEED patterns were observed for the Ge(111), Si(111), and Si(100) surfaces, respectively. Layers of As, Ga, and/or GaAs were then deposited as described below.

The arsenic exposures of the Si and Ge substrates were carried out using the following sequence.

(i) The arsenic-effusion cell was brought up to a temperature that gave a 5×10^{-7} Torr pressure of As_4 molecules in the vacuum chamber.

(ii) The samples were annealed for 10 sec at 850 °C for Si and 730 °C for Ge to desorb any contamination coming from the source as it was warmed up.

(iii) The sample temperature was lowered to the growth temperature of 300 °C to 350 °C and the sample was then turned to face the effusion cell for 10 sec.

(iv) The sample was turned away from the effusion cell and its temperature decreased.

(v) A postanneal to the growth temperature was made after the As_4 pressure in the chamber had dropped into the 10^{-10} Torr range. This anneal did not alter the photoemission spectra with the exception of some small shifts due to changes in band bending.

It should be noted that it is possible that part of the arsenic adsorption took place at temperatures intermediate between the anneal temperature and the growth temperature during the ~60-sec temperature-decrease time. In all cases, the resulting As monolayer was found to be stable for annealing temperature of up to 650 °C.

Gallium exposures were made with a MBE effusion cell and with the sample at room temperature. Ordered structures were obtained by subsequent annealing at 400–500 °C. A high-temperature flashing was carried out to clean the surface prior to the exposure. Films of GaAs were grown using Ga and As_4 effusion cells while holding the substrate temperature 570–580 °C. The GaAs growth rate was limited by the Ga flux and was varied in the range 10^{-2} to 1 monolayers per second.

Angle-integrated photoemission spectra were measured using a cylindrical mirror analyzer (CMA) with its axis at 3.5° from the sample normal and 85° from the incident radiation. The synchrotron radiation was polarized in the plane containing the sample normal, the CMA axis, and the incident radiation. The overall resolution of the grasshopper monochromator and the electron analyzer at $h\nu=130$ eV was less than 0.3 eV full width at half maximum (FWHM).

Core-level spectra were fit to line shapes obtained by convolving Gaussian and Lorentzian functions. All of the fits referred to in this paper used the statistical spin-orbit ratio and a Lorentzian width and spin-orbit splitting energy which were held constant for each core level type. Small variations in the spin-orbit splitting and spin-orbit ratio may arise from final-state effects, but such small changes do not affect the results which we will be discussing. These fixed fitting parameters are given in Table I. The binding energy, intensity, and Gaussian width were allowed to vary.

In order to facilitate the identification of the chemical shifts of the substrate core levels in the case of the GaAs

TABLE I. Input parameters used for fitting the core-level spectra. These parameters were kept fixed for all of the fits described in this paper.

Core level	Spin-orbit splitting Energy (eV)	Intensity ratio	FWHM (eV) Lorentzian	Gaussian
Si $2p$	0.600	1:2	0.075	free
Ge $3d$	0.585	2:3	0.16	free
As $3d$	0.69	2:3	0.16	free
Ga $3d$	0.40	2:3	0.16	free

overlayers, a spin-orbit deconvolution was carried out. Deconvolution into Si $2p_{1/2}$ and Si $2p_{3/2}$ components, for example, requires no curve fitting but is a numerical manipulation of the spectra, having only the spin-orbit splitting and spin-orbit ratio as inputs (again taken as those in Table I). In this method, the intensity $I_0(E)$ of the deconvolved spectrum at a binding energy E is given by

$$I_0(E)=I(E)-rI_0(E-S)\ ,$$

where I is the intensity before deconvolution, S is the spin-orbit splitting, and r is the spin-orbit ratio (r is $\frac{1}{2}$ if the $p_{3/2}$ component is being sought, for example). The subtraction is carried out at one data point after another, starting at a point outside the core level where I_0 and the measured intensity are both zero, and moving in the direction of increasing E. The advantage of a deconvolution such as this is that trends in the data are not hidden by the spin-orbit-associated structure of the spectra.

III. RESULTS AND DISCUSSION

A. Arsenic-terminated surfaces

After arsenic exposures of the Si and Ge substrates, the LEED patterns changed from $c(2\times8)$ to a sharp (1×1) for Ge(111), from (7×7) to a sharp (1×1) for Si(111) and remained as a two-domain (2×1) pattern for Si(100). These results are consistent with the dispersions of the surface states seen previously with angle-resolved photoemission.[5,6,8,10] Core-level spectra for the substrate atoms (Ge $3d$ and Si $2p$) and for arsenic (As $3d$) were measured for all of the surfaces.

The As $3d$ levels for the Si(111):As(1×1), Ge(111):As(1×1) and Si(100):As(2×1) surfaces are shown in Fig. 2 where they are plotted relative to the Fermi energy. In all three cases, a good least-squares fit of the spectrum to a single spin-orbit-split pair was obtained. The solid line in the figure is a result of fitting the data to a single spin-orbit-split pair with a line shape given by convoluting a Lorentzian with a Gaussian function. For the As $3d$ spectrum in Fig. 2, the Gaussian width was found to lie between 0.38 and 0.40 eV. This result shows that it is likely that there is only one site for As atoms on each of the surfaces. Other sites should show up as chemically shifted components. The analogous data for the substrate core levels show only one interface site on each surface.

The substrate core levels for the clean and arsenic-terminated surfaces are shown in Fig. 3. The spectra are aligned at the energy of the bulk Si $2p_{3/2}$ and Ge $3d_{5/2}$ components. For the Si surfaces, the bulk energies were located using bulk-sensitive ($h\nu=108$ eV) spectra and for the Ge(111) surface, values of E_F-E_{VB} obtained earlier[13] with $h\nu=36$ eV were used to check the assignment. The spectra for the arsenic-terminated surfaces have been fitted with two spin-orbit-split pairs using the input parameters given in Table I. Results of the fits are given in Table II. The spectra for the Si(111):As(1×1) surface, which have been described previously,[7] are particularly easy to interpret because of the large chemical shift for Si atoms bonded to arsenic. The shift of 0.75 eV to larger binding energies is greater than the 0.60-eV spin-orbit splitting and allows us to rule out the presence of more than one contribution. Although there is a smaller chemical shift of 0.375 eV for the Ge(111):As(1×1) surface, the Ge $3d$ spectrum can also be fit well with two spin-orbit pairs.

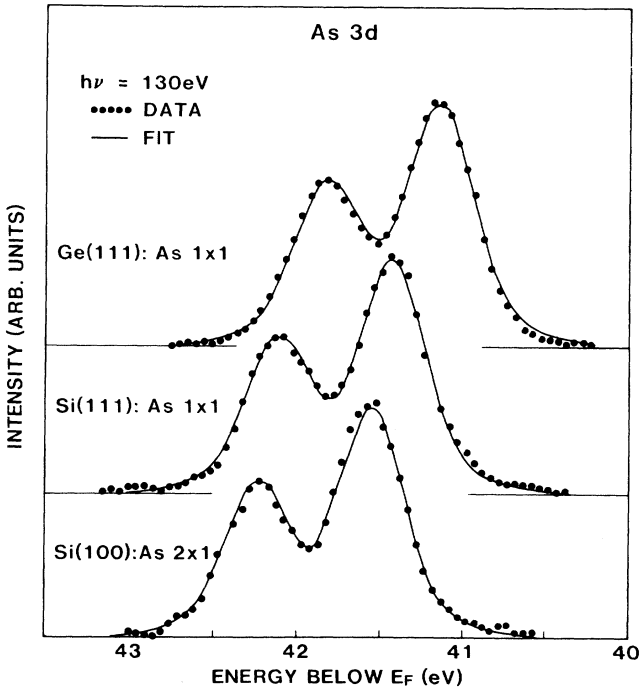

FIG. 2. Arsenic $3d$ core levels for the As-terminated Ge(111), Si(111), and Si(100) surfaces. A fit to a single spin-orbit pair is shown by the curve in each case.

The binding-energy difference between the As $3d_{5/2}$ component and the bulk Si $2p_{3/2}$ component was 58.16 eV for Si(111):As(1×1) and 58.10 eV for Si(100):As(2×1). We find that the separation between the top of the silicon valence band, E_{VB}, and the bulk Si $2p_{3/2}$ energy is 98.82 eV [determined using the value[14] of 0.63 eV for E_F-E_{VB} for Si(111)(7×7)]. This places E_F at 0.75 eV above E_{VB} for Si(111):As(1×1) and 0.83 eV above E_{VB} for Si(100):As(2×1). Similar measurements using $E_{VB}-E(\text{Ge } 3d_{5/2})=29.36$ eV (Refs. 15 and 16) place E_F at 0.13 eV above E_{VB} for Ge(111):As(1×1). These positions of E_F varied by a few tenths of an eV if

TABLE II. Numerical results of fitting the core-level spectra. All energies are given in eV. E_B is the binding energy of the Si $2p_{3/2}$ (Ge $3d_{5/2}$) bulk component. Uncertainties in $E_{VB}-E_F$ are about ±0.1 eV. Δ (eV) is the chemical shift measured from the bulk component (positive values indicate a shift to higher binding energies) and Δ (%) is the percentage of the core-level intensity contained in the shifted component. GW is the Gaussian FWHM measured in eV. The photon energy used was 130 eV in all cases except for the Ge(111):Ga spectrum which was taken at 100 eV.

	Substrate core level					Overlayer core level		
	Δ (eV)	Δ (%)	GW	E_B-E_F	$E_{VB}-E_F$	GW	E_B-E(As $3d_{5/2}$)	E_B-E(Ga $3d_{5/2}$)
Ge(111) $c(2\times8)$	−0.229	56	0.36	29.45	0.09			
	−0.716	8						
Si(111) (7×7)				99.45	0.63			
Si(100) (2×1)	−0.533	17	0.42	99.40	0.58			
Ge(111):As (1×1)	0.375	41	0.36	29.49	0.13	0.40	−12.24	
Si(111):As (1×1)	0.75	40	0.29	99.57	0.75	0.38	58.16	
Si(100):As (2×1)	0.45	60	0.41	99.65	0.83	0.38	58.10	
Ge(111):Ga	−0.312	40	0.39	29.3	0			
Si(111):Ga	−0.330	23	0.41	99.21	0.39	0.38		80.73,80.25,79.87
Si(111):Ga $(\sqrt{3}\times\sqrt{3})$	≤ -0.15		0.42	99.31	0.49	0.38		80.40,80.00,79.56
Si(100):Ga	≤ -0.15		0.45	99.10	0.28			

the samples were exposed to As_4 at room temperature and were restored upon annealing, even though the core-level line shape and intensity did not change noticeably. This indicates that a small fraction (less than 1%) of excess As, missing As atoms, or other adsorbates can vary the band bending.

The relative simplicity of the core-level spectra for the arsenic-terminated (111) surfaces can be contrasted with those for the clean annealed surfaces. For Si(111) (7×7) it was found to be necessary to use four or five spin-orbit pairs to fit the Si $2p$ spectrum if the same width as that obtained for Si(111):As was used. This is not surprising

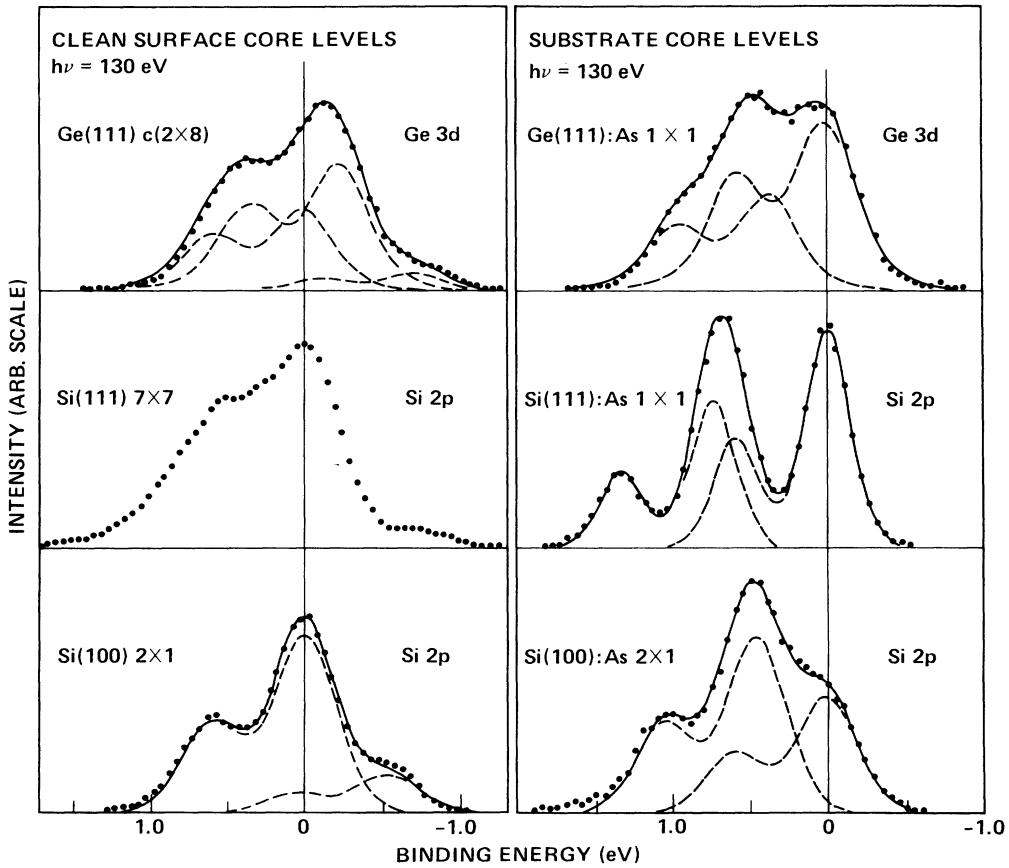

FIG. 3. Si $2p$ and Ge $3d$ core levels for the clean Si(100) (2×1), Si(111) (7×7), and Ge(111) $c(2\times8)$ surfaces and for the same surfaces after they have been terminated with As. The data points are shown by the dots. The dashed lines show the results of deconvolution into bulk Si and chemically shifted components and the full line is the sum of the components. Intensities are shown on an arbitrary scale and the plots are aligned in energy at the bulk level.

considering the many Si sites present in the currently accepted model for this surface.[17] The Ge(111)$c(2\times8)$ surface does not appear from scanning-tunneling microscope data[18] to have distortions as large as those for Si(111)(7×7) and our spectrum can be fitted with two surface-shifted peaks as shown in Fig. 3(a). The directions and magnitudes of the shifts are very close to those obtained previously with different photon energies.[19–21]

The structural model proposed for the arsenic-terminated Si(111) and Ge(111) surfaces[5,7,8] and shown on the left in Fig. 1, has a complete outer double layer with atoms close to bulk-lattice sites. The outer half of this double layer consists entirely of As atoms and the inner half consists entirely of Si or Ge atoms. Each As atom is then in an equivalent site and bonded to three Si (Ge) atoms, consistent with the As $3d$ core-level spectra exhibiting only one component. There are also only two Si or Ge sites: bulk Si(Ge) and interface sites in which each Si(Ge) atom is bonded to three As atoms and to a Si(Ge) atom in the next double layer. This model is also consistent with the Si $2p$ and Ge $3d$ core-level spectra for the Si(111):As(1×1) and the Ge(111):As(1×1) surfaces which show a bulk and a single-interface component.

Surface-state dispersions obtained with angle-resolved photoemission for the Si(111):As(1×1) and Ge(111):As(1×1) surfaces have been compared with those calculated for total-energy-minimized geometries of the model described above.[5,8,22] The agreement is found to be very good and provides additional evidence for the model of the As-terminated (111) surfaces.

Similar results have been presented[6,10] for Si(100):As(2×1). In this case, excellent agreement was found between experimentally determined surface bands and those calculated for an As—As dimer model of the surface. In the model (see Fig. 1), the outer layer of the surface consists of symmetric As—As dimers and the next layer consists of Si atoms close to their bulk sites. This model is consistent with the single component observed for the As $3d$ core-level spectrum. The Si $2p$ spectrum for Si(100):As(2×1) can also be fit with a bulk and a single-interface component. The interface:bulk intensity ratio is 60:40, however, compared with 40:60 for Si(111):As. This difference is probably due to the effect of dimerization of the surface layer. With the experimental geometry used, the CMA accepts electrons emitted at $42°\pm3.5°$ from the surface normal. When the surface atoms dimerize, they pull away from the next-layer atoms. This has the effect of enhancing the measured interface:bulk ratio for Si(100):As and decreasing the surface:bulk ratio for the clean Si(100) surface [the small intensity for the surface component in the Si(100) spectrum can be seen clearly in Fig. 3(a)]. Without such an enhancement, the calculated escape depth for the 25-eV electrons in Si(100):As is 2.5 Å, an anomalously small value.

The core-level data indicate that the arsenic coverage of the Si(100) surface is complete (because of the large shifted intensity for the Si $2p$ level) and that only one type of site exists for As atoms (from the single As $3d$ component seen). A small contribution in the Si $2p$ spectrum also occurs at binding energies of more than 1.5 eV in the region where the fitting is sensitive to background subtraction. It is not clear whether this represents a separate interface contribution, particularly because such a large shift due to As does not seem likely. Contamination due to oxygen would contribute in this region, but was not seen in Auger spectra. Enhanced inelastic scattering is a more likely origin of this signal.

In summary, the arsenic-terminated surfaces show well-characterized As and substrate core levels and are consistent with models for these surfaces proposed on the basis of total-energy calculations and measured surface-band dispersions. The surfaces, which are also chemically inert, were obtained under conditions similar to those at the beginning of MBE growth of GaAs on Si.

B. Gallium-covered surfaces

In contrast to the finding for As-covered Si(111), Ge(111), and Si(100) surfaces, a stable single monolayer of gallium will not form on these surfaces. It is our aim to model the Si—Ga and Ge—Ga bonding which may occur at the GaAs-on-Si and GaAs-on-Ge interfaces, so the stable submonolayer Ga coverages which do occur may not be appropriate. Beginning with a thick (about 3 monolayers) coverage of Ga metal, the Si $2p$, Ge $3d$, and Ga $3d$ core levels were monitored after several annealing steps. The substrate core levels are shown in Fig. 4 for the Ga-covered surfaces after annealing has reduced the thickness to the order of one monolayer. For comparison, results are also shown for the Si(111):Ga$(\sqrt{3}\times\sqrt{3})$ surface which was prepared by depositing a thinner layer of Ga at room temperature followed by a series of anneals at 400–500 °C. Fits to two components are shown for Ge(111):Ga(1×1) and Si(111):Ga(1×1) and to a single component for Si(111):Ga$(\sqrt{3}\times\sqrt{3})$ and Si(100):Ga. It should be noted that the latter two spectra can also be fit with two peaks with a separation of less than 0.1 to 0.15 eV.

The difference between the spectra for Si(111):Ga(1×1) and Si(111):Ga$(\sqrt{3}\times\sqrt{3})$ can be understood when the geometry of the $(\sqrt{3}\times\sqrt{3})$ surface is taken into account. It is now well accepted[23] that each Ga atom is bonded to three Si atoms and each surface Si atom has a "one-third share" of a Ga atom (one Si—Ga bond). The thicker film corresponding to the Si(111):Ga(1×1) spectrum can have Si atoms each bonding to a Ga atom (with the Ga atoms being in the same position as shown for the As atoms in Fig. 1 being one possibility). The chemical shifts observed of 0.330 and up to 0.15 eV in magnitude for Si(111):Ga(1×1) and Si(111):Ga$(\sqrt{3}\times\sqrt{3})$, respectively, are thus consistent with each interface Si atom bonding to a separate Ga atom (with up to three equivalent Si—Ga bonds) for the thicker film. It is not clear which of these bonding arrangements is closest to the situation where Si is bonded to Ga at the Si(111):GaAs interface. We will thus consider both the Si(111):Ga(1×1) and the Si(111):Ga$(\sqrt{3}\times\sqrt{3})$ spectra to represent the possible effects of Si—Ga bonds at the GaAs-on-Si(111) interface.

The small shift on Si(100) is also not unreasonable since each Si has only two Ga—Si bonds at full coverage.

In Fig. 5 we show the Ga 3*d* core levels for the Si(111) surface. The uppermost spectrum was observed after deposition at room temperature. The middle spectrum was obtained after annealing the surface for 2 min at 570 °C, and is the same Si(111):Ga (1×1) surface from which the Si 2*p* core level in Fig. 4 was taken. The spectrum at the bottom is from the surface labeled Si(111):Ga$(\sqrt{3}\times\sqrt{3})+(1\times1)$ in Fig. 4. The three spectra have been aligned relative to the Fermi energy.

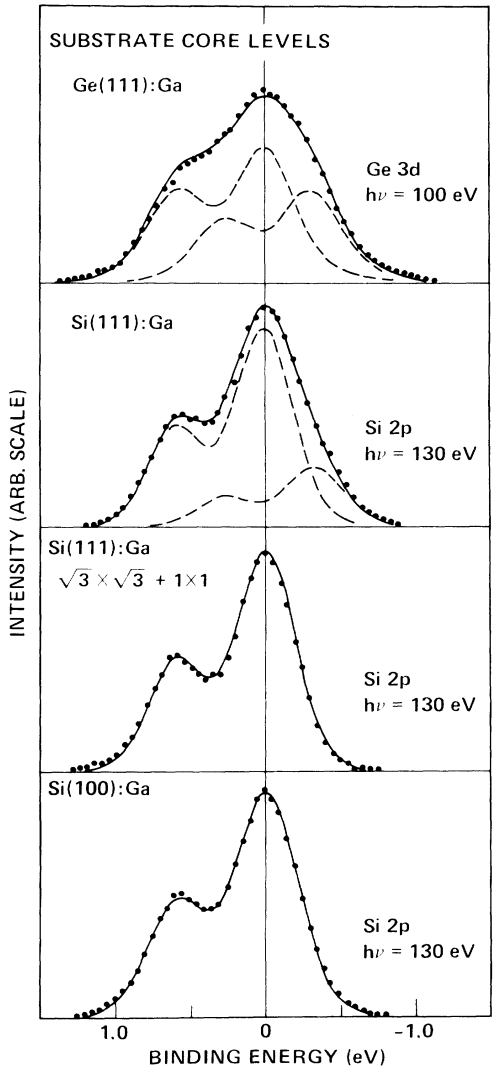

FIG. 4. Si 2*p* and Ge 3*d* core levels for Ga overlayers on the Si(100), Si(111), and Ge(111) surfaces. For Si(111), results are shown both for a thicker film (about one monolayer) and for the Si(111):Ga $(\sqrt{3}\times\sqrt{3})$ surface. The data points are shown by the dots. The dashed lines show the results of deconvolution into bulk Si and chemically shifted components and the full line is the sum of the components. The Si(100):Ga and Si(111) $(\sqrt{3}\times\sqrt{3})$ spectra have been fit with a single spin-orbit component. Intensities are shown on an arbitrary scale and the plots are aligned in energy at the bulk level.

Annealing thick films of Ga on Si(111) is likely to lead eventually to large areas of Si(111):Ga $(\sqrt{3}\times\sqrt{3})$ plus islands of metallic Ga which are far apart and represent only a small fraction of the surface area probed by photoemission experiments.[24,25] Thus the component of the Si(111):Ga (1×1) spectrum at the same energy from the Fermi energy as the metallic Ga peak probably represents regions of metallic Ga. The peaks to greater binding energy then correspond to Ga atoms bonded to one, two, and three Si atoms, respectively. In all cases but the $\frac{1}{3}$-monolayer coverage of Ga (i.e., Ga atoms bonded to three Si atoms), the surface is metallic and it is most appropriate to align the Ga 3*d* spectra relative to the Fermi energy. From the relative intensities of the components, the spectrum labeled Si(111):Ga $(\sqrt{3}\times\sqrt{3})$ appears to have 38% of the Si atoms covered by $\frac{1}{3}$ monolayer of Ga, 32% by $\frac{2}{3}$ monolayer, and 30% by 1

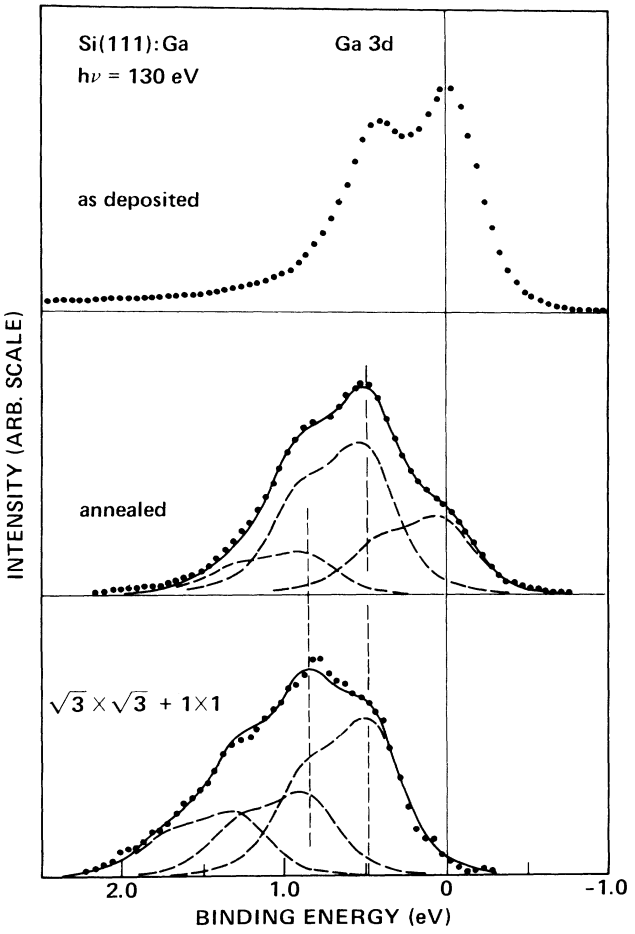

FIG. 5. Ga 3*d* core levels for Ga overlayers on the Si(111) surface. The uppermost spectrum corresponds to a thick metallic layer. The other two spectra were taken from the same Si(111):Ga surfaces as the Si 2*p* data in Fig. 4. The data points are shown by the dots. The dashed lines show the results of deconvolution into different components and the full line is the sum of the components. Intensities are shown on an arbitrary scale and the plots are aligned in energy at the Fermi energy.

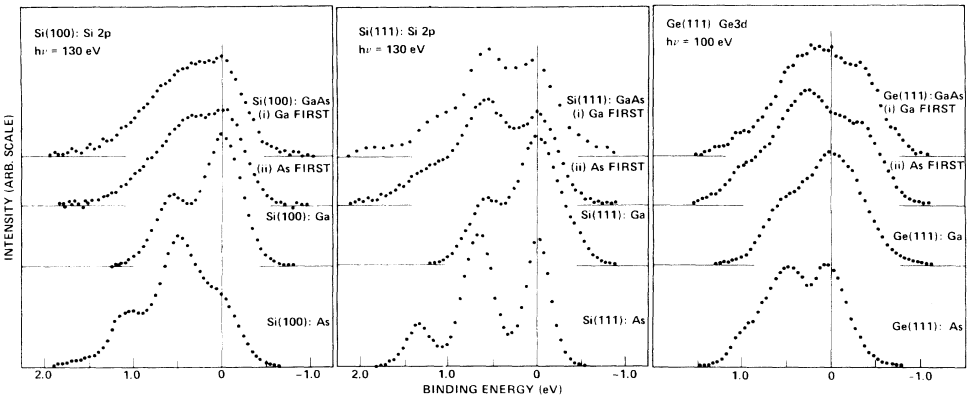

FIG. 6. Si $2p$ and Ge $3d$ core levels for As, Ga, and GaAs overlayers on the Si(100), Si(111), and Ge(111) surfaces. For the GaAs-covered surfaces, results are shown for both As and Ga predeposition. The data points are shown by the dots. Intensities are shown on an arbitrary scale and the plots are aligned in energy at the bulk level.

monolayer. It should be noted that the $\sqrt{3}\times\sqrt{3}$ LEED pattern observed can arise from regions of $\frac{2}{3}$ as well as $\frac{1}{3}$ coverage of Ga.

C. Overview of GaAs-covered surfaces.

Having established the chemical shifts for As alone and Ga alone on the surfaces of interest, we can use these results as a reference in examining the development of thin overlayers of GaAs. The most useful aspect to carry forward in a situation such as this is analysis of the core levels of the substrate atom. There will be many nonequivalent Ga and As sites in the thin overlayers [e.g., As atoms could be bonded to one, two three, or four Ga atoms, be bonded to Si (Ge) or at the surface of the GaAs]. The substrate atoms, however, should only be in bulk or interface sites if interdiffusion does not take place. This is the case even if the GaAs grows as islands in a sea of As-terminated Si or Ge. The first question to answer is whether the interface substrate atoms are bonded exclusively to As, exclusively to Ga, or to both Ga and As. As it is hinted at above, the strong bonding of As to these surfaces would lead us to expect that there would be no bare Si or Ge atoms after the growth has begun. It is known[26,27] that island formation is always found at coverages of less than the order of 100 Å at these growth temperatures for GaAs on Si(100) and so we expect three types of interfaces to occur: (i) Si (Ge) bonded to As alone between islands; (ii) Si (Ge) bonded to thick GaAs (under an island); and (iii) Si (Ge) bonded to a thin layer of GaAs either as the beginning of island formation or as Stranski-Krastanov growth between islands. Because of the surface-sensitive nature of our experiments, we will not detect the interface under thick islands and will observe interfaces of types (i) and (iii).

Figure 6 shows Si $2p$ and Ge $3d$ spectra for thin GaAs layers grown by deposition of Ga in the presence of an As_4 flux on Si(100), Si(111), and Ge(111) compared with those for As alone and Ga alone on the same surfaces. Also shown are spectra for GaAs grown by predepositing Ga at room temperature followed by annealing at 570 °C in a flux of As_4 molecules. Examination of these spectra shows that (i) there are significant differences between the GaAs-covered surfaces and the Ga- and As-covered surfaces and (ii) the GaAs films prepared in the two different ways described above give much the same result. In order to facilitate the identification of the chemical shifts, a spin-orbit deconvolution has been carried out. The spectra shown in Fig. 7 are the resulting Si $2p_{3/2}$ and Ge $3d_{5/2}$ components. We will first describe the results of analyzing the data for GaAs on Si(111) in detail and then discuss GaAs on Si(100) and GaAs on Ge(111).

D. GaAs on Si(111)

Earlier results[28] have shown that for GaAs on Si(111), the substrate core-level spectra resemble most closely those for Si(111):As, indicating that the interface is similar to that shown in Fig. 1. X-ray standing-wave measurements[29] have also shown that the As and Ga atoms occupy the atomic layers consistent with this model. In

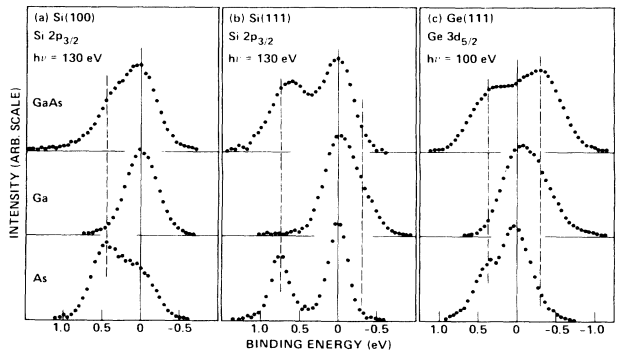

FIG. 7. Si $2p_{3/2}$ and Ge $3d_{5/2}$ core-level components for Si(111), Si(100), and Ge(111) substrates with coverages of approximately one monolayer of GaAs (As first, fast deposition rate), Ga, and As. The vertical dashed lines show the chemical shifts identified for the As-terminated surfaces (higher binding energy) and the Ga-covered surfaces (lower binding energy).

the present work, a variety of deposition conditions were used in order to address the question of how island formation may alter these conclusions. GaAs layers of different thicknesses were deposited onto clean Si(111)(7×7) surfaces while the substrate temperature was held at 570–580 °C. Two different regimes of deposition rates were used, the first being around 1 monolayer per minute to study very thin layers and the second being around 1 monolayer per second in an attempt to reduce the effectiveness of island formation. Results for both sets of data will be examined. As was discussed in the previous section, the best information about interface bonding is likely to come from a detailed examination of the substrate core level.

Figure 7(b) compares the Si $2p_{3/2}$ spectra of Si(111):Ga(1×1) and Si(111):As(1×1) with that of a Si(111):GaAs film grown at the faster rate. As will be discussed below, this film corresponds to a relatively complete coverage of GaAs and allows us to examine the interface bonding in some detail.

The first conclusion that can be drawn from the comparison in Fig. 7 is that the spectrum for the GaAs-on-Si(111) interface appears to be more like that for Si(111):As than for Si(111):Ga. In addition, if the GaAs-on-Si spectrum is decomposed into Si(111):As plus Si(111):Ga components, the Si(111):As component dominates. Any significant contribution from Si(111):Ga would produce more spectral weight in the unshifted peak and/or to lower binding energies, independent of whether the Si(111):Ga(1×1) or Si(111):Ga($\sqrt{3}\times\sqrt{3}$) shift is applicable. For two-dimensional growth of GaAs, this suggests that the interface Si atoms are predominantly bonded to As. We now, however, need to consider whether island formation, which is known to occur[26,27] for thicker films on Si(100), would alter this conclusion. If the islands are thin compared with the probe depth of the experiment or if the area between thick islands is covered by a thin layer of GaAs, then the conclusion remains unchanged. Now we need to examine the situation, shown schematically in Fig. 1, in which the area between islands consists of As-terminated Si. If all of the islands are very thick, then we would see only the Si $2p$ spectrum of Si(111):As(1×1). If at least some of the islands are thin, then we expect the Si $2p$ spectrum to consist of components corresponding to Si(111):As and to Si(111):GaAs. Films were grown at a growth rate of ~1 GaAs bilayer per minute for equivalent coverages varying from ~0.3 bilayer to ~10 bilayers in the low-deposition-rate regime (0.3 bilayers in this context is taken to mean an average coverage of 0.3 layers of GaAs on top of a surface which was initially terminated with a full monolayer of As). Si $2p_{3/2}$ and As $3d_{5/2}$ spectra for some of these films are shown in Fig. 8. Also shown is a spectrum corresponding to around 3 bilayers at the high deposition rate and a spectrum obtained for a surface on which Ga was deposited at room temperature followed by annealing in As.

In order to investigate the effect of island formation, we have fitted the Si(111) $2p$ spectra to a bulk component, a component shifted by 0.75 eV [the chemical shift found above for Si(111):As] and a third component

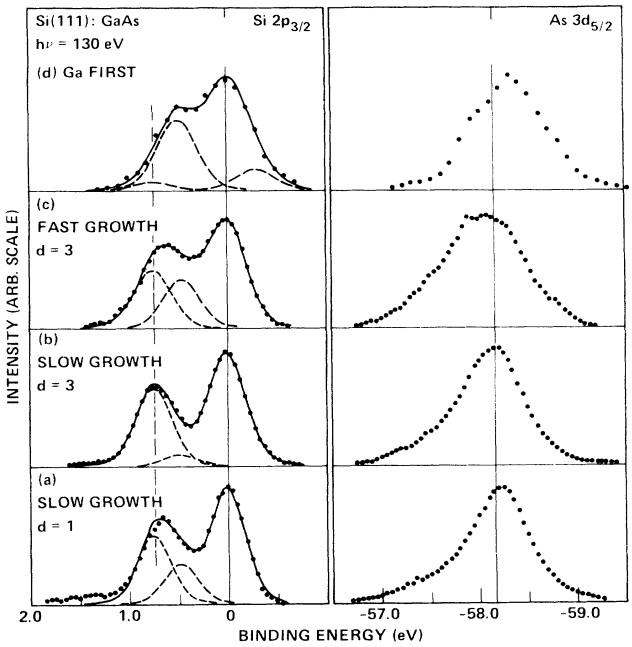

FIG. 8. Si $2p_{3/2}$ and As $3d_{5/2}$ core-level components for a Si(111) substrate with coverages of varying thickness of GaAs. All energies are referenced to the bulk Si $2p_{3/2}$ energy. The Si $2p_{3/2}$ spectra have been fitted with a bulk component (not shown), a component forced to lie at 0.75 eV to higher binding energies, and a third (and fourth, in one case) component which was allowed to vary freely. The full line is the sum of all of the components.

which was allowed to vary freely. All components were required to have the same Gaussian width, and the spin-orbit structure and Lorentzian widths discussed previously. The results of fitting some of the spectra are shown in Fig. 8. For all of the spectra examined, it was found that the third component corresponded to a chemical shift of 0.47±0.03 eV. The magnitude of this shift makes qualitative sense if we assume that the interface consists of islands of GaAs bonded to Si via As atoms and that the area between the islands has the same As-terminated geometry as Si(111):As(1×1). The smaller shift for the Si atoms bonded to GaAs can arise because the As atoms at the interface are bonded to Ga as well as Si atoms, so that their ability to pull electrons from the Si atoms is reduced.

The relative intensities of these components of the Si $2p$ spectra are also consistent with this picture of the interface. We expect that the growth begins by the addition of an As—Ga bilayer on top of the Si(111):As surface. If we now postulate that this continues until a fractional coverage Θ is achieved and then growth takes place on top of the already covered regions, we can predict the behavior of the Si $2p$ core-level components. The number of Si atoms bonded to As—Ga—As will increase relative to the number bonded to As alone until the fractional coverage reaches Θ. At this point, the growth in thickness of the islands, although not altering the bonding of the interface Si atoms, will reduce the observed intensity of the Si:GaAs signal relative to the

Si:As signal.

Calculation of the expected Si:GaAs to Si:As intensity ratio was carried out as a function of Θ using this islanding model of the growth. Results for an escape depth of 6.5 Å for the Si $2p$ core level (photoelectron kinetic energy of around 25 eV) are shown as an example in Fig. 9. Comparison with the experimental results in Fig. 9 shows that $\Theta \approx 0.6$ fits the data at the lower coverages but not at the higher coverages when the effect of lateral growth of the islands (not included in the calculation) becomes important. This value of Θ was also found to be consistent with the variation of the As $3d$ to Si $2p$ total intensity ratio. By using values for the effective escape depth of the photoelectrons in the range 4 to 7 Å, values of Θ were found to fall in the range 0.6 to 0.8.

For the GaAs film grown at the faster rate we see in Fig. 8 that there is a much larger fraction of the Si:GaAs component in the spectrum than there was at similar coverages at the slower growth rate. The corresponding value for Θ is greater than 0.9, or less than 10% of the surface being uncovered by GaAs. This is consistent with the total area between islands being reduced at the faster growth rate. In further analysis of the interface bonding, we will use the data for the faster growth rate because more of the Si:GaAs interface can be seen in the spectra.

The As $3d_{5/2}$ spectra in Fig. 8 are also consistent with island formation. The spectra are aligned at the bulk Si $2p_{3/2}$ energy and the vertical line at 58.16 eV above that energy corresponds to the separation seen for Si(111):As. The spectrum in (a) shows a large As $3d_{5/2}$ component near 58.16 eV and a contribution at around 0.5 eV to higher binding energies. This contribution is greatest in (c), suggesting that it corresponds to As at the interface. The two components in (d) which lie above and below 58.16 eV may represent surface As on GaAs and As in bulk GaAs sites, because the Si $2p$ spectrum from this film shows that there is almost complete coverage of GaAs.

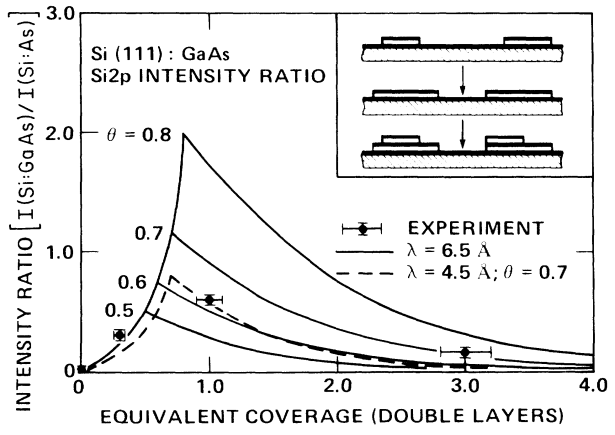

FIG. 9. Calculated ratio of GaAs-shifted Si $2p$ intensity to As-shifted intensity for a model (shown in the inset) of the growth in which GaAs islands form on a Si(111):As substrate after a coverage of Θ bilayers has been reached. Atomic layers of As and Ga atoms are shown as black and white regions, respectively, in the inset and the Si substrate is shown as the shaded region. Values are given for a range of Θ for an electron escape depth, λ, of 6.5 Å and the dashed curve shows the result for $\lambda = 4.5$ Å and $\Theta = 0.7$. Experimental intensity ratios are shown for films of different equivalent thickness grown at the slower growth rate.

The formation of islands at the beginning of GaAs-on-Si epitaxy is probably a direct result of the passivation effect that the As overlayer has on Si(111). It has been found, for example, that the As-terminated surface is $\sim 10^{11}$ times less reactive with oxygen molecules than is the Si(111)(7×7) surface.[8] The As atoms on Si(111):As are fully coordinated, and so bonding of the arriving Ga atoms is not as favorable as it is for Ga on the surface of GaAs where the As atoms are not fully coordinated. Ga atoms which arrive on the As-terminated areas of the surface appear to have sufficient lateral mobility to diffuse to the islands before bonding.

One way to avoid the clustering that leads to island formation is to reduce the effectiveness of the As termination by beginning the growth with a uniform Ga coverage and then adding As atoms. As can be seen in Fig. 6, this procedure gives the qualitatively similar result that most of the shift is in the "As direction," implying that the bonding is still predominantly to As atoms. This means that the As atoms go underneath the Ga atoms to bond to the Si substrate. Our results are consistent with those for GaAs grown on Si(100) where it was found[30] that predepositing Ga at a coverage of less than one monolayer leads to the same GaAs orientation as does predeposition of As. Analysis of the Si $2p_{3/2}$ spectrum shown in Fig. 8 for the Ga-first growth showed that only small contributions ($\sim 5-10\%$) arise from Si bonded to Ga or As alone and that the 0.47- to 0.75-eV intensity ratio is about 8. This corresponds to almost complete coverage of GaAs.

E. Si(100):GaAs

The core-level spectra for the GaAs-covered Si(100) surface show that the growth of GaAs on Si(100) has some features in common with that on Si(111) but also significant differences As was the case for the Si(111) substrate, the spectra for Si(100):GaAs grown with As first or Ga first are very similar to one another and are distinctly different from those for Si(100):As or Si(100):Ga (see Fig. 6). In contrast to the changes seen as a function of thickness for Si(111):GaAs, the Si $2p_{3/2}$ spectra for GaAs on Si(100) (some of which are shown in Fig. 10), showed little change. Spectra were measured for equivalent thicknesses of 0.3 to 10 bilayers of GaAs and the Si $2p_{3/2}$ data were fitted in two ways: (i) assuming the presence of only one shifted peak and (ii) assuming a fixed shift for Si(100):As and the presence of a second shifted component [a similar method to that shown for the (111) surface in Fig. 8]. Because the chemical shifts of the Si $2p$ level by both As and Ga overlayers are smaller for Si(100), the fits were less definitive and both of these fitting schemes yielded fits of similar quality. Numerical results of both methods for approximately one bilayer are given in Table III.

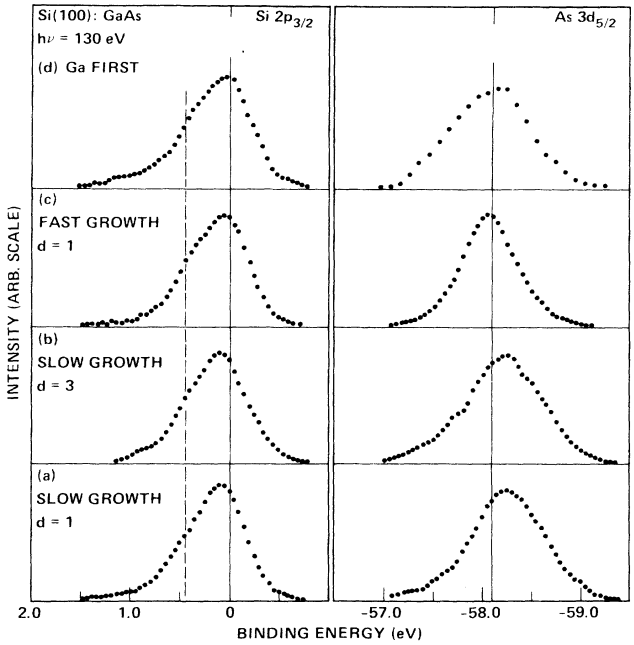

FIG. 10. Si $2p_{3/2}$ and As $3d_{5/2}$ core-level components for a Si(100) substrate with coverages of varying thickness of GaAs. All energies are referenced to the bulk Si $2p_{3/2}$ energy and the vertical dashed lines show the chemical shifts identified for the Si(100):As surface.

Fitting all of the Si(100):GaAs spectra to a bulk and a single shifted peak yielded similar chemical shifts (0.39±0.02 eV) and similar intensities in the shifted component (0.35±0.08 of the total intensity). The simplest interpretation of the result is that the surface is completely covered by GaAs and that the interface consists of Si—As bonds with a shift of 0.39 eV. The fact that there is a small shift for Ga on Si(100) suggests that both Si—As and Si—Ga bonds could be present with the latter intensity being coincident with the bulk Si $2p$ peak. These two possibilities can be separated by examining the relative intensities of the shifted and unshifted components. We consider, for example, the Si(100):GaAs spectrum in Fig. 7(a) which corresponds to the fast deposition rate. It is possible to synthesize a spectrum similar to the Si(100):GaAs spectrum by adding the Si(100):As and Si(100):Ga spectra, shown in Fig. 7(a), in the ratio of 3:2. As was discussed in Sec. III A, the As-shifted component for Si(100):As (2×1) is anomalously intense because the As—As dimer formation pulls the As atoms away from the interface Si atoms (as seen by the cylindrical mirror electron-energy analyzer) and over the next-layer Si atoms. When the GaAs overlayer breaks the As—As dimers bonded to Si, this enhancement will disappear. Using a 40% contribution for the As-shifted component of the Si $2p$ core level [the same amount as for Si(111):As (1×1)] and then synthesizing the Si(100):GaAs spectrum from Si(100):As and Si(100):Ga components requires less than around 20% of the interface to have Si—Ga bonds. This result does not change significantly if we use the 0.45-eV shift for As on Si(100) or the 0.39-eV shift for the Si—As—Ga—As shift inferred above from fitting the Si(100):GaAs spectra to a single shifted peak.

In the second fitting method, analogous to the scheme used for Si(111):GaAs, it was found that if a chemical shift of 0.45 eV [corresponding to the shift for Si(100):As] was input, a third component was found at an energy shifted from the bulk component by 0.13±0.03 eV to higher binding energies. This large reduction of the interface Si $2p$ chemical shift on going from a coverage of As to a coverage of As—Ga—As compared to the result for Si(111) can be understood from the different atomic geometries. When the GaAs layer is formed in the (100) case, the As atoms bonded to Si lose both one bond to an As atom and a lone pair while gaining two bonds to Ga. On the Si(111) surface, on the other hand, the As atoms lose only the lone pair and gain a single bond to Ga. The intensity of the third component only varied from 20% to 24% of the total intensity for the thickness range studied. This indicates that island formation (with areas of As-terminated Si between the islands) is not so dominant on Si(100) as on Si(111):GaAs. A similar analysis of island formation to that discussed for Si(111):GaAs was carried out. The smaller shifts in the (100) case make this less reliable, but we were able to place a lower limit of 50% for the island coverage of the surface at equivalent coverages of around one bilayer.

TABLE III. Numerical results of fitting the substrate Si $2p_{3/2}$ ($h\nu=130$ eV) and Ge $3d_{5/2}$ ($h\nu=100$ eV) core-level spectra for GaAs films grown using the fast As-first method (spectra shown in Fig. 7). Δ (eV) is the chemical shift measured from the bulk component (positive values indicate a shift to higher binding energies) and Δ (%) is the percentage of the core-level intensity contained in the shifted component. GW is the Gaussian FWHM measured in eV. The shifts marked with * were held fixed during the fitting procedure.

	Two shifted peaks			One shifted peak		
	Δ (eV)	Δ (%)	GW	Δ (eV)	Δ (%)	GW
Ge(111):GaAs	−0.37	42	0.43	0.606	43	0.54
	0.396	28	0.43			
Si(111):GaAs	0.46	23	0.41	0.63	45	0.63
	0.75*	28	0.41			
Si(100):GaAs	0.16	20	0.45	0.39	37	0.47
	0.45*	34	0.45			

This last result appears to be in contradiction with the cross-sectional transmission electron microscope (TEM) studies by Hull and Fischer-Colbrie[27] of the beginning of GaAs epitaxy on Si(100) which showed that island formation occurs with around 90% of the surface being between islands at equivalent coverages of 10 Å. If this is the case, then our results imply that, unlike the results for Si(111):GaAs discussed above, the area between islands must be covered with GaAs layers. Coverage with As alone between such widely spaced islands would lead to a spectrum very similar to the Si(100):As (2×1) spectrum which can be seen in Fig. 7(a) to look qualitatively different from that for Si(100):GaAs. It is possible that a single GaAs layer would not be seen in TEM, particularly after the sample has been thinned. Hull and Fischer-Colbrie also find that the islands appear to nucleate at steps on the Si(100) substrate. Our data for on-axis Si(100) substrates could lead to different nucleation conditions.

Examination of Fig. 1 shows that the presence of any single-atom steps on the Si(100) substrate will lead to antiphase domains (APD's) in the GaAs if the interface bonding remains constant. It has been found[11] that off-axis Si(100) substrates can lead to the absence of APD's. An earlier study of such substrates[10] showed that double-height atomic steps predominate and that a monolayer of As could form without disrupting the step structure. This provides a simple explanation of the avoidance of APD's on off-axis Si(100).

F. Ge(111) GaAs

Results are shown in Figs. 6 and 7 for GaAs layers grown on Ge(111) at the faster deposition rate. As was the case for GaAs layers on Si(100) and Si(111), there is a strong similarity between the results for the As-first and the Ga-first depositions. The Ge(111) case is different in that the substrate seems to be bonded to both As and Ga. We have no accurate method of determining the energy of the bulk component in the GaAs-on-Ge spectra. The width of the GaAs-on-Ge spectra can be seen to be significantly greater than that for either Ge(111):As or Ge(111):Ga. It is possible to fit the Ge(111):GaAs spectrum with a bulk plus either one or two shifted components (results are given in Table III). With a single shifted component the shift found is 0.61 eV, which is far greater than the As-only shift of 0.375 eV. This suggests that there are at least two shifted components present. The alignment of the spectra in Figs. 6 and 7 is the result of fitting to three components, one shifted by 0.40 eV to higher binding energies from the bulk component and one by 0.37 eV to lower binding energies. These values are close to those given in Table II for bonding to As alone and Ga alone, suggesting that the Ge(111):GaAs spectrum contains contributions from Ge—As and Ge—Ga bonds.

The question now arises of why there is an apparent difference in the interface bonding for Ge(111):GaAs where there seems to be comparable bonding to Ga and As and no evidence of island formation, and Si(111):GaAs where most bonding seems to be to As and where island formation is an important effect. It has been found[31] that considerable intermixing occurs for the case of relatively thick Ge on GaAs surfaces. Intermixing has also been seen[32] for coverages of around one monolayer of Si on GaAs. The Ge(111)$c(2\times8)$ surface begins to melt[33] at 300 °C, while the Si(111)(7×7) surface does not disorder[34] until 870 °C, making it likely that the degree of intermixing between Ge and GaAs is greater than that between Si and GaAs at the growth temperature of 570 °C.

IV. SUMMARY AND CONCLUSIONS

Arsenic bonds strongly to the Si(111), Si(100), and Ge(111) surfaces studied here. The core-level line-shape analysis shows a single As site and a single substrate interface site in all cases. The substrate core level exhibits a well-defined chemical shift to higher binding energy in all cases. These results further support the geometries proposed previously for these surfaces.[5–8] For Ga overlayers the substrate core-level shifts are found to be to lower binding energies for Si(111):Ga(1×1) and Ge(111):Ga and to be small for Si(111)$(\sqrt{3}\times\sqrt{3})$ and Si(100):Ga.

GaAs overlayers on the same substrates show substrate core-level line shapes which are distinctly different from those for As or Ga alone. The shapes, however, are found to be rather independent of whether Ga or As prelayers were used in the GaAs growth.

We find that the majority of the bonds at the interface take place between Si and As atoms for GaAs on both Si(111) and Si(100). Interdiffusion was found to be greater for the Ge(111):GaAs and both Ge—As and Ge—Ga bonds were found. For an equilibrium situation, Harrison *et al.*[9] have suggested that equal numbers of Si—As and Si—Ga bonds should be present in order to reduce a dipole at the surface. At greater GaAs thicknesses than those considered here, dislocations will be introduced as the lattice mismatch can no longer be accommodated by straining the overlayer. Although it is possible that this will allow some solid-phase rebonding to take place at the interface, it seems unlikely at the growth temperatures used. It should be kept in mind that MBE is a nonequilibrium process and at very thin overlayers the lowest-energy equilibrium geometry may not occur in practice. The question of the effect of the surface dipole on the interface bonding is still unresolved and requires further investigation.

Formation of GaAs islands, with As-terminated Si between the islands, is seen to be more dominant on Si(111) than on Si(100) at similar GaAs coverages. This may indicate that the reactivity of Si(111):As is lower than that for Si(100):As. An islanding model is shown to represent the qualitative behavior of the Si $2p$ core levels for GaAs on Si(111). For Si(100):GaAs we are unable to distinguish between island growth on a bilayer of GaAs and fairly uniform two-dimensional growth. The islanding seen in TEM investigations,[26,27] suggests that the former explanation may be correct. An extension of the present study to growth on stepped surfaces is necessary to establish whether surface steps are dominating the nu-

cleation seen in TEM.

The ability to suppress island formation has important implications for the growth of thick GaAs films on Si as the presence of islands at the beginning of growth leads to poor surface morphology of the film. We have shown for the case of GaAs on Si(111) that the total area between islands can be reduced either by using faster deposition rates or by growing with submonolayer Ga prelayers.

ACKNOWLEDGMENTS

We are grateful for many discussions with J. E. Northrup, D. K. Biegelsen, R. M. Martin, and D. J. Chadi, and for the skillfull assistance of L. E. Swartz. Part of this work was performed at the Stanford Synchrotron Radiation Laboratory which is supported by the Department of Energy Office of Basic Energy Sciences.

---

*Present address: Department of Physics, University of California, Berkeley, CA 94720.

†Present address: Department of Physics and Measurement Technology, Linköping Institute of Technology, S-581 83 Linköping, Sweden.

[1]R. Fischer, N. Chand, W. Kopp, H. Morkoc, L. P. Erikson, and R. Youngman, Appl. Phys. Lett. **47**, 397 (1985).

[2]Y. Itoh, T. Nishioka, A. Yamamoto, and M. Yamaguchi, Appl. Phys. Lett. **49**, 1614 (1986).

[3]T. H. Windhorn and G. M. Metze, Appl. Phys. Lett. **47**, 1031 (1985).

[4]R. D. Dupuis, J. P. van der Ziel, R. A. Logan, J. M. Brown, and C. J. Pinzone, Appl. Phys. Lett. **50**, 407 (1987).

[5]R. D. Bringans, R. I. G. Uhrberg, R. Z. Bachrach, and J. E. Northrup, Phys. Rev. Lett. **55**, 533 (1985); J. Vac. Sci. Technol. A **4**, 1380 (1986).

[6]R. I. G. Uhrberg, R. D. Bringans, R. Z. Bachrach, and J. E. Northrup, Phys. Rev. Lett. **56**, 520 (1986); J. Vac. Sci. Technol. A **4**, 1259 (1986).

[7]M. A. Olmstead, R. D. Bringans, R. I. G. Uhrberg, and R. Z. Bachrach, Phys. Rev. B **34**, 6041 (1986).

[8]R. I. G. Uhrberg, R. D. Bringans, M. A. Olmstead, R. Z. Bachrach, and J. E. Northrup, Phys. Rev. B **35**, 3945 (1987).

[9]W. A. Harrison, E. A. Kraut, J. R. Waldrop, and R. W. Grant, Phys. Rev. B **18**, 4402 (1978).

[10]R. D. Bringans, R. I. G. Uhrberg, M. A. Olmstead, and R. Z. Bachrach, Phys. Rev. B **34**, 7447 (1986).

[11]See, for example, R. Fischer, H. Morkoc, D. A. Neumann, H. Zabel, C. Choi, N. Otsuka, M. Longerbone, and L. P. Erikson, J. Appl. Phys. **60**, 1640 (1986).

[12]Ludox WP colloidal silica, E. I. Dupont De Nemours and Co.

[13]R. D. Bringans, R. I. G. Uhrberg, and R. Z. Bachrach, Phys. Rev. B **34**, 2373 (1986).

[14]F. J. Himpsel, G. Hollinger, and R. A. Pollak, Phys. Rev. B **28**, 7014 (1983).

[15]R. W. Grant, E. A. Kraut, S. P. Kowalczyk, and J. R. Waldrop, J. Vac. Sci. Technol. B **1**, 320 (1983).

[16]E. A. Kraut, R. W. Grant, J. R. Waldrop, and S. P. Kowalczyk, Phys. Rev. B **28**, 1965 (1983).

[17]K. Takayanagi, Y. Tanishiro, M. Takahashi, and S. Takahashi, J. Vac. Sci. Technol. A **3**, 1502 (1985); Surf. Sci. **164**, 367 (1985).

[18]R. S. Becker, J. A. Golovchenko, and B. S. Swartzentruber, Phys. Rev. Lett. **54**, 2678 (1985).

[19]S. B. Di Cenzo, P. A. Bennett, D. Tribula, P. Thiry, G. K. Wertheim, and J. E. Rowe, Phys. Rev. B **31**, 2330 (1985).

[20]R. D. Schnell, F. J. Himpsell, A. Bogen, D. Rieger, and W. Steinmann, Phys. Rev. B **32**, 8052 (1985).

[21]A. L. Wachs, T. Miller, A. P. Shapiro, and T.-C. Chiang, Phys. Rev. B **35**, 5514 (1987).

[22]M. S. Hybertsen and S. G. Louie, Phys. Rev. Lett. **58**, 1551 (1987).

[23]See, for example, J. M. Nicholls, B. Reihl, and J. E. Northrup, Phys. Rev. B **35**, 4137 (1987).

[24]See, for example, the discussion for Ag on Si(111) by J. A. Venables, J. Vac. Sci. Technol. B **4**, 870 (1986).

[25]D. Bolmont, P. Chen, C. A. Sebenne, and F. Proix, Surf. Sci. **137**, 280 (1984).

[26]D. K. Biegelsen, F. A. Ponce, A. J. Smith, and J. C. Tramontana, J. Appl. Phys. **61**, 1856 (1987).

[27]R. Hull and A. Fischer-Colbrie, Appl. Phys. Lett. **50**, 851 (1987).

[28]R. D. Bringans, M. A. Olmstead, R. I. G. Uhrberg, and R. Z. Bachrach, *Proceedings of the 18th International Conference on the Physics of Semiconductors*, edited by O. Engström (World Scientific, Singapore, 1987), p. 191; Appl. Phys. Lett. **51**, 523 (1987).

[29]J. R. Patel, J. A. Golovchenko, P. E. Freeland, M. S. Hybertsen, and D. C. Jacobson (unpublished).

[30]T. Won, G. Munns, R. Houdré, and H. Morkoc, Appl. Phys. Lett. **49**, 1257 (1986).

[31]R. S. Bauer and H. W. Sang, Jr., Surf. Sci. **132**, 479 (1983).

[32]R. Z. Bachrach, R. D. Bringans, M. A. Olmstead, and R. I. G. Uhrberg, J. Vac. Sci. Technol. B **5**, 1135 (1987).

[33]R. J. Phaneuf and M. B. Webb, Surf. Sci. **164**, 167 (1985).

[34]P. A. Bennett and M. B. Webb, Surf. Sci. **104**, 74 (1981).